American Mineralogist, Volume 67, pages 360–372, 1982

The modulated structure of cubic Cu_9BiS_6

KAZUSHIGE TOMEOKA[1]

Mineralogical Institute, Faculty of Science
University of Tokyo, Hongo, Tokyo 113, Japan

AND MASAAKI OHMASA

Institute of Material Science
University of Tsukuba
Sakura-mura, Ibaraki 305, Japan

Abstract

Quenched single crystals synthesized at about 550°C in the compositional region about Cu_9BiS_6 were found to reveal non-integral type satellite reflections. These superstructure peaks have been studied in detail. The substructure obtained using only main reflections is cubic, space group $Fm3m$, with $a = 5.563(1)$Å; and it has a structure similar to cubic α-chalcocite. Through analysis of the partial Patterson function, the superstructure of the material was found to consist of periodically spaced clusters of Bi and Cu, which are alternately distributed according to a face-centered cubic arrangement. The superstructure shows good agreement between observed and calculated intensities. The repeat distance and the regularity of the long-range ordering appear to change with crystal composition; these observations can be explained on the basis of the structure obtained in this study. The same kind of modulated structure is observed in another quenched material $Cu_3Bi_5S_9$, in the Cu_2S–Bi_2S_3 system. At high temperature, these phases exist with a disordered metal distribution, and the metal clusters of both materials are considered to be produced during quenching from high temperature.

Introduction

The first systematic studies on the phase relations of the Cu_2S–Bi_2S_3 join were carried out independently by Sugaki and Shima (1971, 1972) and Buhlmann (1971). Their phase diagrams coincide except in the region between Cu_2S (chalcocite) and Cu_3BiS_3 (wittichenite), where Sugaki and Shima recognized an independent phase, Cu_9BiS_6, but Buhlmann found only a broad solid solution range of Cu_2S instead. Sugaki and Shima reported that Cu_2S and Cu_9BiS_6 had similar structures at high temperature, and it was difficult to distinguish between them in the X-ray powder patterns. Quenched products rarely retained the phases present at run temperature, and those quenched from above 400°C usually showed several weak additional peaks.

As is well known, chalcocite, Cu_2S, has three quite different polymorphs, stable at different temperatures. γ-chalcocite, which is stable up to about 103°C, is monoclinic and has a very complicated crystal structure based on hexagonal close packing of sulfur atoms (Evans, 1971; 1979). β-chalcocite, which is stable between 103° and 435°C, is the high-temperature form of the γ-chalcocite and is also based on a hexagonal close packing. Copper atoms in the β-chalcocite are distributed statistically into their tetrahedral and trigonal sites (Wuensch and Buerger, 1963; Sadanaga et al., 1965). On the other hand, α-chalcocite, which is stable above 435°C, has a structure in which sulfur atoms are cubic close packed, and copper atoms occupy their tetrahedral interstices (Morimoto and Kullerud, 1966). If the compounds close to Cu_2S composition in the Cu_2S–Bi_2S_3 system retain the β- and α-chalcocite structures, as suggested by the previous investigators, it is clear that there remains no site that can accommodate such a large atom as Bi other than an octahedral hole in the close packed sulfur framework. If that is true, however, Bi and Cu cannot occupy adjacent sites at the same time, because of

[1]Present address: Department of Geology, Arizona State University, Tempe, Arizona 85287.

0003–004X/82/0304–0360$02.00

the restriction of distance between the two atoms. Thus it was presumed that some kind of statistical replacement occurs between the two atoms, as observed in some other compounds in this system (Ohmasa, 1973; Ozawa and Nowacki, 1975; Tomeoka *et al.*, 1980). Further, we thought it might also be possible that some kind of long range periodic structure would occur, due to the substitution between Bi and Cu, as seen in $Cu_3Bi_5S_9$ (Ohmasa *et al.*, 1979).

We synthesized single crystals having compositions close to Cu_9BiS_6 by quenching from above 500°C. The quenched materials have been found to reveal two different kinds of interesting higher order structures. One of them has the substructure corresponding to the cubic α-chalcocite, and the other has the substructure corresponding to the hexagonal β-chalcocite. The structural problems of the former[2] will be discussed in detail in the present paper.

Experimental

Synthesis and identification

The cubic phase was obtained by quenching from 550°C, after being kept at that temperature for two months. The mixing ratio of the starting elements was Bi : Cu : S=1 : 9 : 6. The starting materials were granular copper of 99.99% purity, bismuth metal of 99.99% purity, and sulfur as guaranteed reagent by Wako Pure Industries, Ltd.. These elements were sealed into an evacuated silica tube. A closely fitting glass rod was inserted into the tube to minimize the vapor volume.

The quenched specimens were studied with single crystal X-ray techniques. The crystals reveal fundamental reflections corresponding to a cell edge with a = 5.54–5.56Å and a face-centered cubic lattice. Many non-integral type extra reflections (satellite reflections) occur in clusters, around the fundamental reflections. A single-crystal X-ray precession photograph of (110) is shown in Figure 1, and the three-dimensional diffraction pattern is drawn schematically in Figure 2. The precession photograph (110) of the cubic phase (Fig. 1) is reminiscent of that of digenite or bornite (Donnay *et al.*, 1958; Morimoto and Kullerud, 1966), but the appearance of the extra reflections is quite different. The extra peaks of digenite and bornite are located along the lines between the main reflections, whereas those of our material appear in clusters near the main reflections only and do not exist midway between them. As seen in Figure 1, the X-ray diffraction pattern of the cubic phase has several remarkable features. These are described as follows:

(1) The satellite reflections are not located at simple fractions of the reciprocal cells. Instead their period corresponds to a non-integral multiple of the subcell. This period varies in the range of 6.0–6.75.

(2) The satellites form a three-dimensional, body-centered, cubic reciprocal lattice centered about the main reflections (Fig. 2).

(3) Generally the intensities of the satellites are strong, and some of them are stronger than those of the main reflections.

(4) As compared with the main reflections, the satellites are slightly diffuse; degree of diffuseness differs from sample to sample.

(5) The asymmetry of intensities between pairs of satellites centered about the main reflections is remarkable. Generally, the intensities of lower angle satellites are stronger than those of higher angle ones, and this tendency is emphasized as the indices become higher.

While investigating the quenched specimens by X-ray diffraction techniques, we found that different crystals show slight differences in the X-ray diffraction features described above. Three representative samples 1, 2 and 3 are compared in Table 1. By comparing these features, it is clear that there is a correlation among the distance between satellite reflections, the sharpness of the satellite spots, and the length of the fundamental cubic cell edge.

Substructure determination

Taking the view that the substructure would provide useful information about the higher order structure, we tried to determine the substructure, using only the main reflections. The intensities of the main reflections were collected for sample 2 on an automatic 4-circle diffractometer (Syntex $P2_1$), by ω-2θ scan, using Mo$K\alpha$ radiation monochromated by graphite. Reflections with intensities less than 2σ were excluded as unobserved. A total of 34 reflections were finally obtained and were corrected for Lorentz and polarization factors, and for absorption (μ = 317.7 cm^{-1}), using the program ACACA (Wuensch and Prewitt, 1965).

If this substructure were basically similar to α-Cu_2S, as mentioned previously, copper atoms

[2]This material will be noted as "cubic phase" after this. The problem of the latter will be presented elsewhere.

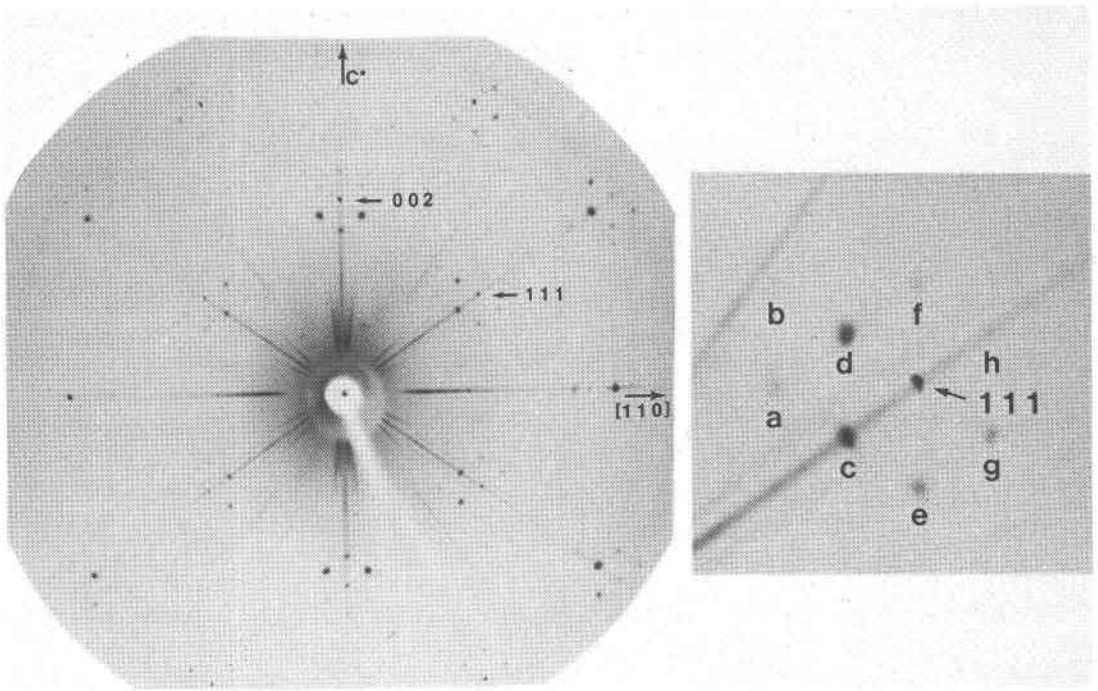

Fig. 1. A precession photograph of (110) of the cubic phase, with enlargement of the area about the 1, 1, 1 reflection. The satellite reflections around 1, 1, 1 are: a: $1-2\delta, 1-2\delta, 1$; b: $1-2\delta, 1-2\delta, 1+2\delta$; c: $1-\delta, 1-\delta, 1-\delta$; d: $1-\delta, 1-\delta, 1+\delta$; e: $1, 1, 1-2\delta$; f: $1, 1, 1+2\delta$; g: $1+\delta, 1+\delta, 1-\delta$; h: $1+\delta, 1+\delta, 1+\delta$; δ: 1/6.5–1/6.75 of distances between the main reflections.

would be situated in the tetrahedral holes formed by cubic close packing of sulfur atoms, and bismuth atoms would prefer the larger octahedral holes. At the initial stage, we assumed that sulfur atoms occupy the nodes of a face-centered cubic lattice, and bismuth and copper atoms occupy the centers of the octahedra and the tetrahedra respectively. Based on these atomic positions, the least squares method was employed, varying the occupancies and isotropic temperature factors, and the R factor was reduced to 18%. The temperature factors of bismuth and copper were unusually large. At this stage, in difference Fourier maps, additional positive peaks were found near the centers of triangular faces of the sulfur tetrahedra. This suggested two possibilities. One is that a small amount of copper should simply be introduced to the new sites, the centers of triangular faces of the sulfur coordination tetrahedra; the other possibility is that copper atoms in the centers of the tetrahedra should be redistributed and shifted in four different directions, perpendicular to each triangular face of the tetrahedra, as observed in the high temperature form of digenite (Morimoto & Kullerud, 1963). Both cases were individually applied, but the R-factor was not improved substantially. However, the combination of both cases greatly improved the agreement of FO and FC and reduced the R factor to 7.3%. After the refinements, the anomaly in the difference Fourier maps disappeared. The least squares calculations were carried out with the full matrix least squares program LINUS (Coppens and Hamilton, 1970). Scattering factors for neutral atoms from the *International Tables for X-ray Crystallography* (1968) were used. Corrections for anomalous dispersion were employed for all atoms using the values by Cromer (1965). Chemical composition derived from the results of the refinement is $Cu_{8.06}Bi_{0.83}S_6$. Lattice parameters and atomic parameters of sample 2 are listed in Table 3 and Table 2 respectively, and the atomic arrangement in the substructure is schematically illustrated in Figure 3.

Discussion of the structure

Before beginning a discussion on the higher order structure, we should consider the results obtained in the foregoing experiments. The X-ray diffraction patterns indicate that there exists some modulation wave in the structure, the period of which corre-

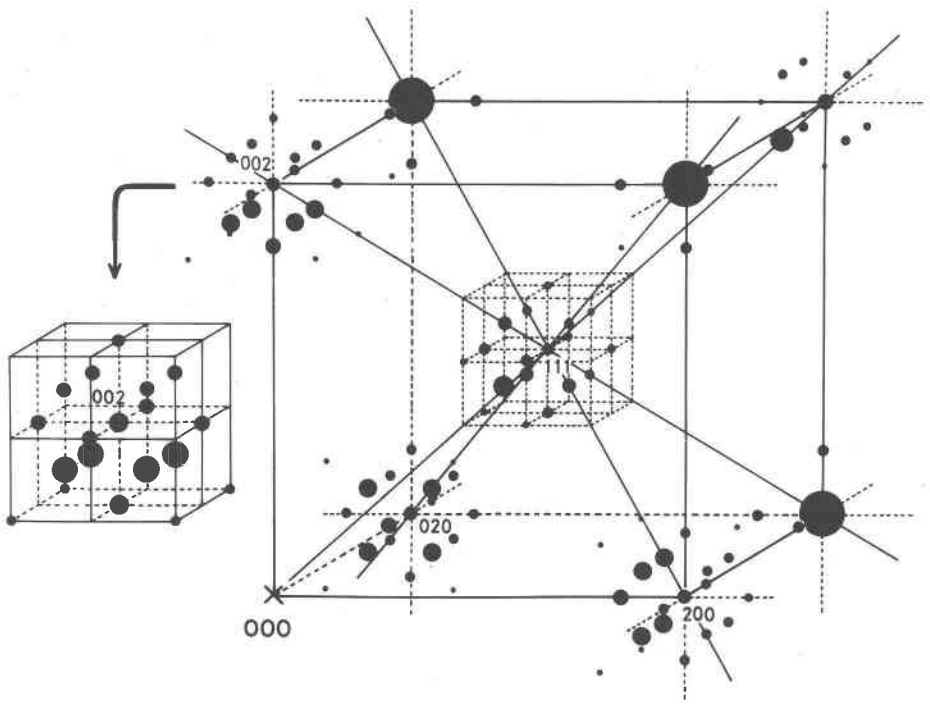

Fig. 2. Schematic diagram showing the three-dimensional distribution of the reflections in an octant of reciprocal space.

sponds to a non-integral multiple of the subcell between 6.0 and 6.75. The higher order structure is due to a three dimensional periodicity and consists of a face-centered cubic lattice. The broad satellite reflections in contrast to the sharp main reflections may indicate that the periodicity of the long-range ordering is not as exact as that of the fundamental subcell.

Some characteristics found in the substructure provide information on the higher order structure; one is an unusually large temperature factor for the Bi atoms, and another is a complicated statistical distribution of Cu atoms (Fig. 3). In view of the fact that the substructure is a result of averaging over the whole structure, these features suggest large displacements of the atoms, as will be discussed later.

It should be noted that even if Bi and Cu occupy different sites in the sulfur arrangement, they cannot occupy adjacent sites at the same time, because the Cu–Bi distances are too short. Therefore, a replacement between the two atoms should occur, as observed in other compounds in the Cu_2S–Bi_2S_3 system: cuprobismuthite (Ozawa & Nowacki,

Table 1. Characteristics of diffraction patterns of the cubic phase modifications

Sample	Cell dimension (Å)	Distance* between satellites	Degree of sharpness of satellites
1	5.549(1)	1/6.0	low
2	5.563(1)	1/6.5	medium
3	5.564(1)	1/6.75	high

* *expressed by fractions of distances between main reflections.*

Table 2. Atomic parameters of the substructure of sample 2

Atom	Occupancy	x	y	z	B_i
Bi	0.138(4)	0.5	0.5	0.5	4.86(41)
Cu1	0.109(2)	0.2787	0.2787	0.2787	1.59(21)
Cu2	0.059(4)	0.3333	0.3333	0.3333	2.47(40)
S	1.0	0.0	0.0	0.0	1.45(7)

1975), $Cu_3Bi_5S_9$ (Ohmasa, 1973) and $CuBi_3S_5$ (Tomeoka *et al.*, 1980). If this is true, the higher order structure found in this material might be attributed to the periodic substitution between Bi and Cu, as observed in $Cu_3Bi_5S_9$ (Ohmasa *et al.*, 1979). The strong intensities of the satellite reflections can probably be explained as due to the periodic replacement between Bi and Cu, which have a large difference in scattering factors.

Furthermore, as observed by Guinier (1963), the asymmetry of intensities between pairs of satellites, which is one of the remarkable characteristics of the cubic phase, suggests that the modulation of the replacement of atoms accompanies a modulation having the same period of the positional parameters of the atoms.

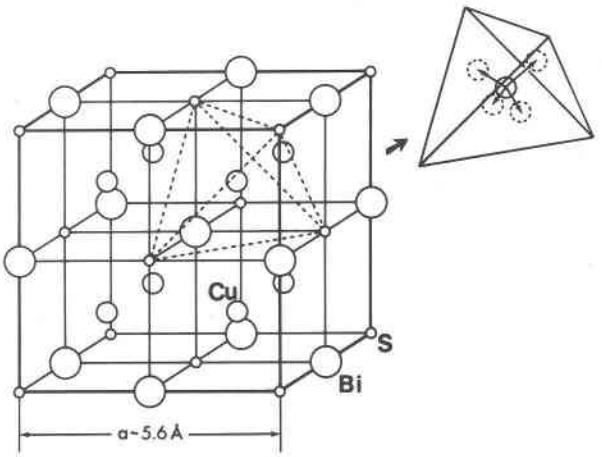

Fig. 3. Atomic arrangement of the substructure. A statistical distribution of copper atoms in only one tetrahedron of sulfur atoms (shown by broken lines) is illustrated.

Superstructure investigation

If the higher order structure is due to some kind of modulation, as mentioned above, we can recognize the non-integral repeat distance as a period corresponding to a modulation wave. If we consider a superstructure with a proper integral multiple of the substructure, the non-integral period in the actual structure can be conveniently approximated by this integral period. We adopted sample 2 (6.5*a* type) to investigate the superstructure using X-ray diffraction intensity data, because the period (6.5 multiple of subcell) can be made integral (13 multiple of subcell) simply by doubling the 6.5.

For convenience of crystallographic calculations, we initially assumed the superstructure to have the space group, *Fm*3*m*, because the satellite reflections form a body-centered cubic lattice in reciprocal space and they satisfy *m*3*m* point symmetry. We can now examine the actual structure as a superstructure having a lattice constant $a' = 13a = 72.32$Å and a cubic face-centered lattice. The crystal data of sub- and superstructure are listed in Table 3.

Table 3. Crystal data of the sub- and superstructure

Substructure	Superstructure
a' = 5.563 ± 0.001 Å	a = 13×a' = 72.32 ± 0.01 Å
Fm3m	Fm3m
z = 1 ($Cu_{5.378}Bi_{0.552}S_4$)	z = 2197

Intensities of the satellite reflections were collected for sample 2 (6.5*a* type), on the 4-circle diffractometer by ω-2θ scan, up to 100° in 2θ, using Cu$K\alpha$ radiation monochromated by graphite. After corrections of Lorentz and polarization factors and absorption, a total of 97 satellite reflection data were obtained.

Patterson function

If the modulation is based on the replacement between Bi and Cu as mentioned previously, it was presumed that the replacement should have a substantial effect on the partial Patterson function, obtained only from the satellite reflections, because there is a large difference in the scattering power between the two atoms. In Figure 5a and 5b, Patterson sections of $Z = 0$ and $Z = 1/52$ ($1/4a'$ of the subcell), calculated using program GSFFR (Ohmasa, 1973), are drawn. As seen from both figures, it is remarkable that the sharp positive and negative peaks appear in clusters. The positive peaks are located near the positions that correspond to the centers of octahedra of sulfur, and the negative peaks occur near the centers of tetrahedra. Both kinds of clusters of the peaks are periodically distributed three-dimensionally around the points that correspond to the equipoints 4a, 4b and 24d of *Fm*3*m* (Wyckoff notation) in the supercell.

Several workers have so far succeeded in applying the partial Patterson function to solve superstructures. Among them, Koch and Cohen (1969) employed the function to analyze the non-integral

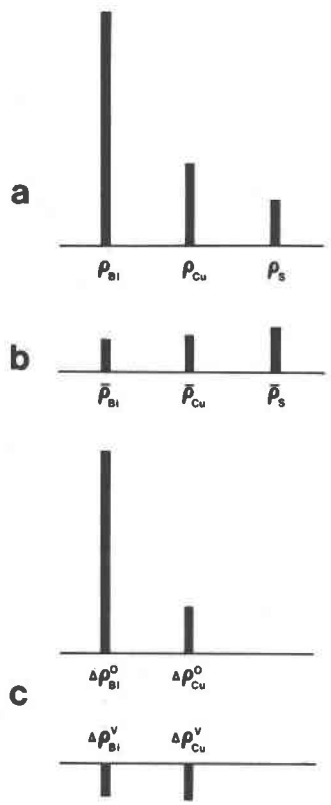

Fig. 4. Electron density peaks. a: real peaks. b: peaks in the average structure, $\bar{\rho}$(average). c: peaks in the difference structure, $\Delta\rho = \rho$(super)–$\bar{\rho}$(average).

type superstructure of wüstite, $Fe_{1-x}O$. The modulation of wüstite is composed of repeated clusters of Fe atoms and of Fe atom defects, which can be regarded in another sense as the periodic substitution between Fe and vacancies (whose scattering factor is considered to be zero). In our case, the superstructure can actually be considered to have four kinds of metal sites; *i.e.*, occupied Bi, vacant Bi, occupied Cu and vacant Cu sites. Therefore, the mode of the substitution of the atoms is much more complicated; in fact, the substitution does not occur exactly on the same position for Bi and Cu, but at the different positions between both the metal atoms and vacancies.

Provided that the electron density peak height is simply proportional to the atomic number, the real electron density peaks and the peaks in the average structure, which are given by multiplying the atomic numbers by their occupancies, can be illustrated as vertical bars in Figure 4a and 4b. Electron density peaks of each site in a hypothetical "difference structure", which are obtained by subtracting the peaks of the average structure from the real peaks, *i.e.*, $\Delta\rho = \rho$(superstructure)-$\bar{\rho}$(average structure), are illustrated in Figure 4c. The peaks of the positions occupied and unoccupied by metal atoms correspond to the positive electron density bars and the negative bars in Figure 4c, respectively. Consequently, the Patterson function can be interpreted as a set of interatomic vectors between these peaks in the hypothetical "difference structure" (Frueh, 1953; Takeuchi, 1972). This function should have positive peaks corresponding to positive electron density pairs or negative pairs, and negative peaks corresponding to positive and negative electron density pairs. Several possible pairs of these hypothetical peaks, being supposed to produce fairly high peaks on the Patterson maps, are listed in Table 4 in peak height order. As noted from the list, we can see that $\Delta\rho^o_{Bi}$–$\Delta\rho^o_{Bi}$ would overwhelmingly contribute to the positive peaks on the Patterson maps, whereas $\Delta\rho^o_{Bi}$–$\Delta\rho^v_{Cu}$ and $\Delta\rho^o_{Bi}$–$\Delta\rho^v_{Bi}$ would contribute to the negative peaks.

If the large positive peaks observed in Figure 5a can mainly be attributed to the ends of $\Delta\rho^o_{Bi}$–$\Delta\rho^o_{Bi}$ interatomic vectors, then Bi atoms can be considered to form clusters distributed on the equipoints of 4a, 4b and 24d of $Fm3m$ in the superstructure unit cell; specifically, the peaks are due to the products of those vectors between the Bi atoms of each Bi cluster which spans the distance between each equipoint. Two of the vectors corresponding to a positive peak A of the $Z = 0$ Patterson section (Fig. 5a) are denoted by solid arrows in the actual structure (Fig. 5c). Because Cu sites are vacant within the Bi clusters, the $\Delta\rho^o_{Bi}$–$\Delta\rho^v_{Cu}$ vectors are produced

Table 4. Interatomic vectors in the partial Patterson function

Positive peaks		Negative peaks
$\Delta\rho^o_{Bi} - \Delta\rho^o_{Bi}$	$\Delta\rho^v_{Cu} - \Delta\rho^v_{Bi}$	$\Delta\rho^o_{Bi} - \Delta\rho^v_{Cu}$
$\Delta\rho^o_{Bi} - \Delta\rho^o_{Cu}$	$\Delta\rho^v_{Bi} - \Delta\rho^v_{Bi}$	$\Delta\rho^o_{Bi} - \Delta\rho^v_{Bi}$
$\Delta\rho^o_{Cu} - \Delta\rho^o_{Cu}$		$\Delta\rho^o_{Cu} - \Delta\rho^v_{Cu}$
$\Delta\rho^v_{Cu} - \Delta\rho^v_{Cu}$		$\Delta\rho^o_{Cu} - \Delta\rho^v_{Bi}$

o : *occupied*
v *vacant*

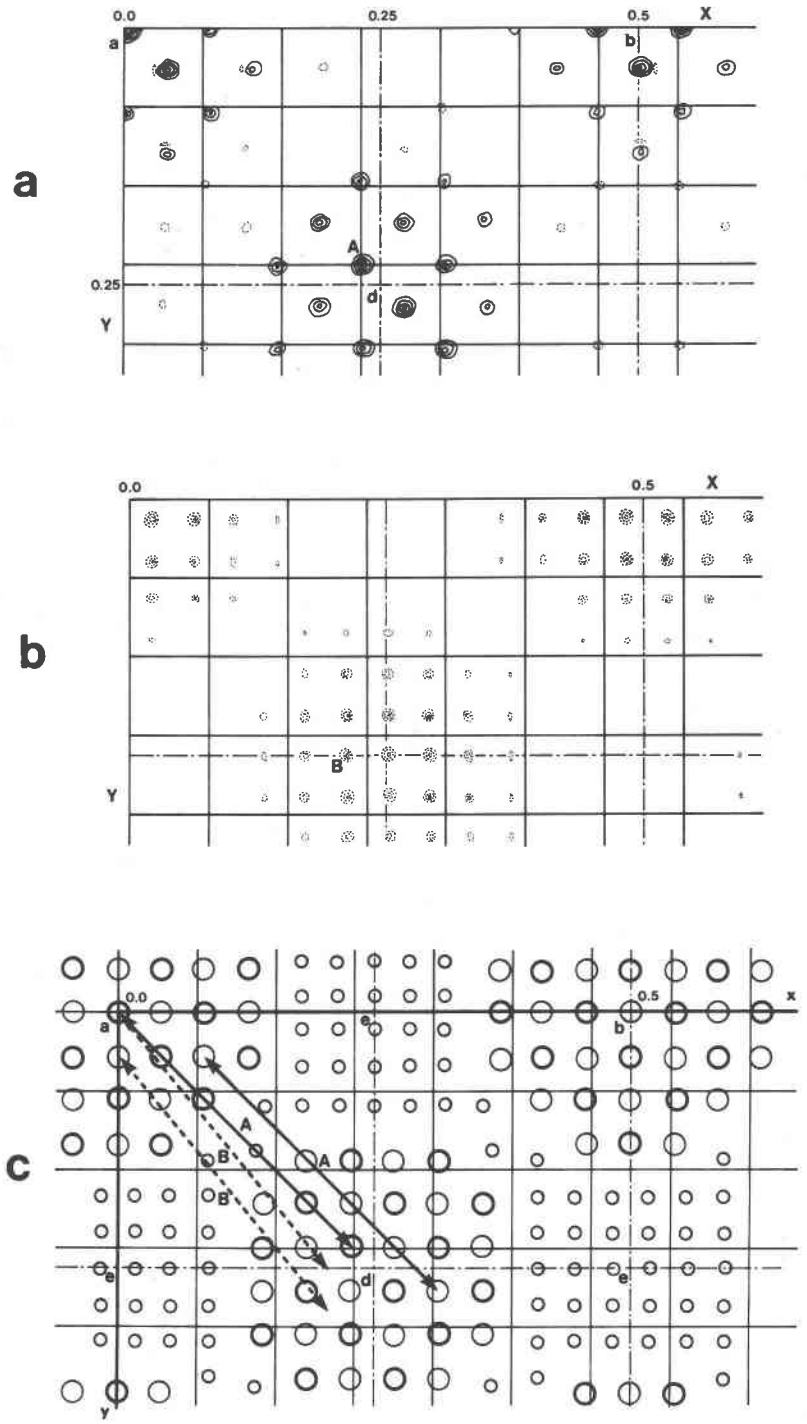

Fig. 5. Partial Patterson sections (a, b) and the finally derived structure (c). a: partial Patterson section of $Z = 0.0$. Contours of peaks are drawn at arbitrary intervals. Solid contours indicate positive peaks and broken contours negative peaks. One square block corresponds to one subcell. Equipoints a, b and d of $Fm3m$ are indicated. b: partial Patterson section of $Z = 1/52$, corresponding to a section of $Z = 1/4a'$ (a': cell edge length of subcell). Negative peaks are clustered around equipoints a, b and d. c: two of $\Delta\rho^{\circ}_{Bi} - \Delta\rho^{\circ}_{Bi}$ and of $\Delta\rho^{\circ}_{Bi} - \Delta\rho^{v}_{Cu}$ interatomic vectors are indicated by solid arrows and broken arrows in the finally derived structure (refer to Fig. 7). The former vectors correspond to the positive peak A denoted in the Patterson section $Z = 0.0$ (a), and the latter vectors correspond to the negative peak B in the section Z = 1/52 (b). Note that the displacement of Bi and Cu is demonstrated in this figure, although displacement distances do not equal the real values.

and also span the distance between each equipoint. The negative peak clusters, as observed in the Patterson section, $Z = 1/52$, can therefore be interpreted as corresponding to the products of these interatomic vectors. Two of the vectors corresponding to a negative peak B of the Patterson section, $Z = 1/52$ (Fig. 5b), are denoted by broken arrows in Figure 5c. Thus far, the interpretation of the partial Patterson function suggests that the superstructure is basically composed of metal atom clusters that are arranged according to a face-centered cubic lattice (Fig. 5c).

Another remarkable feature of the Patterson map is that the large positive peaks are without exception displaced from the ideal centers of the octahedral sites in directions radially outward from the central point of each cluster of peaks (Fig. 5a). In addition, the distances of the displacements appear to be proportional to the distances between the peaks and the center of each cluster. If the large positive peaks correspond to the interatomc vectors of Bi atoms, as described above, this fact may suggest that Bi atoms shift outward from the centers of the clusters.

Construction of the model

At this stage, we have the general outline of the superstructure and can now derive a detailed model of the structure. An initial model was constructed as follows: S atoms are considered to be arranged according to face-centered cubic close packing. Bi atoms are made to occupy the octahedral sites in the sulfur packing and to group in clusters equally around each equipoint of 4a, 4b and 24d of *Fm3m*. On the other hand, Cu atoms are made to occupy the tetrahedral sites and to occur in areas in which the Bi atoms do not exist. Then those Cu atoms can be regarded as forming Cu clusters being distributed on the equipoints of 8c and 24e. As a result, each Bi and Cu complex in the superstructure unit cell is distributed alternately as if it were one of the atoms in a NaCl type structure.

Because the periodicity of the superstructure is incommensurate with that of the substructure, and because the asymmetric unit of the superstructure has far too many atoms (Table 5), it is very difficult to construct a model satisfying exactly such high symmetry conditions as those imposed by *Fm3m*, especially if we consider the displacement of atoms. Therefore, although the initial model satisfies exactly such high symmetry, the model was modified to the lower symmetry orthorhombic space group *Fmmm* to avoid such difficulties and complications in constructing models. Reflections equivalent under *Fm3m* were checked at each stage of calculating the structure factors, but the discrepancies produced due to the difference of the space groups were very small and can be neglected in the present models.

Table 5. Number of atoms contained in the superstructure

Atom	Occupancy (%)	Subcell	Supercell	1/32 of supercell*
Bi	13.8	0.55	1210	38
Cu1	10.9	3.49	7660	239
Cu2	5.9	1.89	4150	130
S	100.0	4.0	8788	275

* *which corresponds to an asymmetric unit of the orthorhombic cell.*

From the knowledge of the chemical composition derived from the substructure determination, total numbers of atoms within an asymmetric unit of the superstructure can be estimated as indicated in Table 5. The Bi clusters are distributed on the *Fm3m* equipoints 4a, 4b and 24d according to cubic close packing. The relative position of each equipoint with respect to the array of sulfur atoms is different, which results in three different kinds of Bi clusters. Initial arrangement of these possible Bi clusters within 1/32 of the superstructure unit cell is illustrated in Figure 6. Next, Cu atoms were distributed in the centers of sulfur tetrahedra around the equipoints 8c and 24e of *Fm3m*. In the placement of Cu, care was taken that the distances between Bi and Cu were not shorter than 3.2Å, which is considered to be the shortest limit of the distance between the two atoms. If the space occupied by Bi atoms is eliminated from the asymmetric unit, there remains space to accommodate about 350-380 Cu atoms, which agrees well with the number, 369 (Table 5), determined from the chemical composition.

Structure factor calculation

Starting from this basic model, we refined the structure to improve the agreement of FO and FC. Unfortunately, the model has far too many atoms (more than 20000 atoms) in a unit cell to use

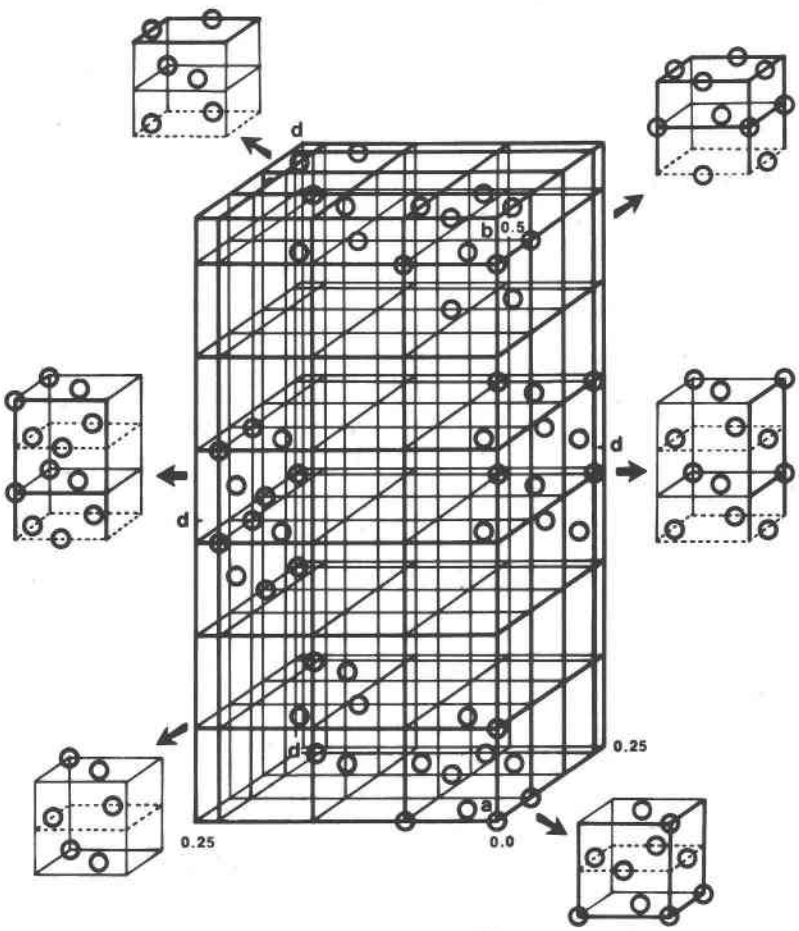

Fig. 6. Initial arrangement of Bi clusters within 1/32 of the superstructure unit cell. Three kinds of Bi clusters, being distributed in equipoints a, b and d of $Fm3m$, are indicated.

ordinary least squares or Fourier methods in refining the structure with only at most 111 intensity data, of which 14 are from the main reflections. As a result, we had to adopt the trial and error method to refine the structure. Fortunately, as mentioned in earlier sections, we already have useful information that suggests how the structure should be modified from the starting model. Based on the initial arrangement of the atoms described above, the structure factors were calculated. The temperature factors used in the calculation were the same as those obtained in the subcell determination. The initial R factor obtained by adjusting only the scale factor was 56%.

First, the effect of the displacements of the atoms was considered. The large temperature factor of Bi in the substructure can be attributed to the large displacements of the atoms. On the partial Patterson map the high positive peaks, which are considered to be products of interatomic vectors between Bi atoms, are slightly displaced outward from the centers of the positive peak clusters, strongly suggesting that Bi atoms are displaced outward from each center of the Bi complexes.

The complicated statistical distribution of Cu atoms can also be understood as a result of this shift modulation. The mode of their distributions indicates that Cu atoms do not move at random, but shift in four definite directions from the center of the tetrahedron of sulfur atoms toward the centers of the triangular faces (Fig. 3). Contrary to the case of Bi, Cu atoms would shift from the central positions of the tetrahedra inward toward the centers of the Cu clusters.

The positions of S atoms are also affected by the movement of the metal atoms. The sulfur atoms in

the regions of each metal cluster will move in approximately the same direction as the metal atoms.

An increase in the sizes of the metal complexes was suggested by Bragg-Lipson diagrams, based on several reflections whose FO and FC showed considerable disagreement in the initial structure factor calculation. This modification greatly improved the agreement of FO and FC. Increasing the number of sites contained in each cluster requires the occupancies of the metal sites to be reduced, because the total number of metal atoms in one cluster is constant. At the same time, this means that the effect of statistical replacement between Bi and Cu should be introduced into the superstructure model. Thus, the Bi and Cu clusters do not always alternate regularly through the entire crystal, but are disordered to some extent. Although this disorder seems to be unusual at first sight and to make the structure more complicated, the broadening of the satellites can be attributed to such a lack of periodicity in the metal cluster distribution.

The structure factors for each structure model, which we modified by the trial and error method, were calculated. Thus, we finally reached a structure that gives substantial agreement between FO and FC. The final unweighted reliability factor is 26.9%. Comparison between FO and FC is demonstrated in Table 6.

Table 6. Observed and calculated structure factors

	h	k	l	Fo	Fc		h	k	l	Fo	Fc
	0	0	22	11.0	23.5	*	13	13	13	10.3	8.0
*	0	0	26	19.4	20.3		13	13	17	5.1	3.3
	0	0	30	8.0	4.3		13	13	35	13.2	14.1
	0	0	48	21.5	15.1	*	13	13	39	19.5	19.8
*	0	0	52	60.7	65.1		13	13	61	10.6	7.8
	0	0	56	6.3	1.6	*	13	13	65	9.0	12.1
	0	0	74	10.6	11.9		13	35	35	7.1	5.5
*	0	0	78	18.3	18.1		13	35	39	8.6	7.8
	0	0	82	4.9	2.9		13	35	61	7.1	3.5
	0	4	26	8.8	9.3		13	39	61	6.7	3.9
	0	4	48	7.6	2.1	*	13	39	65	14.8	16.6
	0	22	22	9.9	6.3		15	15	37	17.3	6.6
	0	22	26	13.7	9.3		15	15	41	7.5	5.8
	0	22	48	4.1	6.5		15	33	37	3.1	1.2
	0	22	52	7.2	6.6		15	37	37	8.5	5.3
	0	22	74	6.4	4.1		15	37	59	2.9	2.1
*	0	26	26	113.2	127.4		18	18	26	3.5	1.8
	0	26	30	4.2	3.0		22	22	48	4.7	1.9
	0	26	48	12.2	15.2		22	22	52	4.3	1.6
*	0	26	52	12.5	8.1		22	26	26	10.4	12.2
	0	26	74	11.7	8.0		22	26	48	8.4	5.0
*	0	26	78	23.0	22.9		22	26	52	6.0	2.4
	0	48	48	10.3	7.4		22	48	48	4.6	1.8
	0	48	52	9.0	5.0		24	24	24	43.5	30.8
*	0	52	52	41.3	41.8		24	24	28	17.6	13.8
	2	2	24	28.7	25.7		24	24	46	5.3	2.2
	2	2	28	9.1	8.1		24	24	50	8.7	16.4
	2	2	76	11.8	8.1		24	24	72	4.2	2.1
	2	20	50	2.5	2.5		24	24	76	13.2	11.0
	2	24	50	26.0	18.5		24	28	28	6.5	3.7
	2	24	72	4.1	2.4		24	50	50	19.1	15.6
	2	24	76	6.0	7.5		24	50	54	4.2	2.7
	2	28	50	13.8	7.9		26	26	30	3.7	2.4
	2	50	50	8.8	10.7		26	26	48	14.6	8.5
	4	4	22	2.5	4.1	*	26	26	52	52.1	51.1
	9	13	13	8.2	11.9		26	26	74	8.8	7.7
	9	13	35	8.1	3.7		26	48	48	4.6	5.7
	9	13	39	8.7	5.8		26	48	52	5.7	5.5
	9	13	61	5.0	2.9		26	48	56	4.8	1.9
	9	17	17	3.2	2.9	*	26	52	52	7.6	4.4
	9	35	61	3.1	1.1		28	28	76	5.9	2.3
	9	39	61	4.8	1.4		28	50	50	10.1	7.7
	11	11	11	15.6	18.4		33	37	37	2.9	2.9
	11	11	15	16.3	13.7		35	35	35	6.0	2.4
	11	11	33	5.1	2.5		35	35	39	8.0	2.9
	11	11	59	4.9	3.7		35	35	61	3.0	1.9
	11	11	63	9.9	2.9		35	39	39	6.8	3.9
	11	15	15	7.4	10.9		35	39	61	3.0	1.6
	11	15	37	9.2	8.7		37	37	37	10.6	4.5
	11	15	41	6.3	5.2		37	37	41	5.1	1.6
	11	15	59	4.1	1.8		37	37	59	3.6	3.5
	11	15	63	8.0	1.9		37	41	41	5.2	2.1
	11	33	37	3.5	2.9	*	39	39	39	30.9	30.6
	11	37	37	19.4	7.8		48	48	48	8.3	2.6
	11	37	41	9.5	3.2		48	48	52	6.2	3.0
	11	37	59	3.8	3.7						

*Indices marked by * indicate the main reflections.*

The final structure

The arrangement of each atom in the finally refined structure can be described as follows:

Bi atoms. The Bi atoms occupy octahedral interstices in the sulfur packing and locally make a rocksalt-like structure with S atoms. Three kinds of Bi complexes, A, B and D, are distributed on the equipoints a, b and d of *Fm*3*m*, as indicated in Fig. 7. Occupancies of Bi sites of each complex are 43.7%, 41.3% and 39.6% respectively. The isotropic temperature factor is 3.5 for all atoms. The atoms are displaced radially outward from the centers of the complexes.[3] The displacement distances equal the distances between the centers of the complexes and the centers of the Bi octahedral sites, multiplied by 0.035.

Cu atoms. The Cu atoms in the initial model are tetrahedrally coordinated by four sulfur atoms and locally form a structure similar to α-chalcocite (or the high-temperature form of digenite). However, on account of some kind of atomic interaction, they are markedly displaced, and those situated on the centers of tetrahedral faces can be considered as a result of extreme displacement. We distinguished between tetrahedrally coordinated Cu and triangularly coordinated Cu in calculating structure factors. The former that occur in the regions of the Bi complexes, within 9.8Å of the center of a complex, are given occupancies of 20.0%, and are displaced in the same directions as the Bi atoms. The remaining Cu atoms in tetrahedral sites are distributed about the equipoints 8c and 24e of *Fm*3*m*. Their

[3]The displacement mode of Bi and Cu is demonstrated in Fig. 5c, although displacement distances are exaggerated.

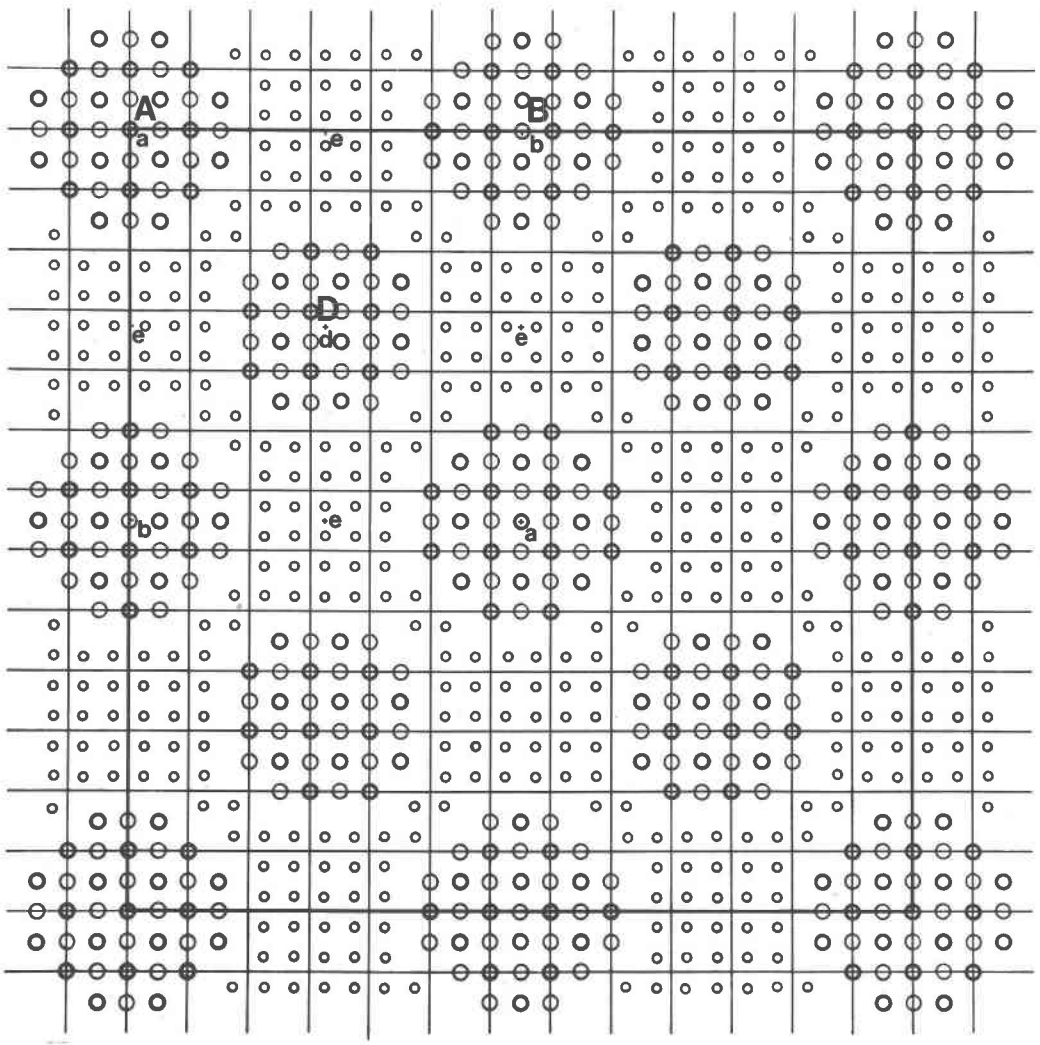

Fig. 7. The arrangement of the metal atoms in the finally derived superstructure. Displacement of the atoms is disregarded. This corresponds to a projection of Bi and Cu, which are situated between $z = -1/26$ and $z = 1/26$ (corresponding to the levels $z = \pm 1/2a'$ (a': cell edge length of subcell). Large thick circles and large thin circles indicate Bi atoms on the level $z = 0.0$ and those on the level $z = -1/26$ or $1/26$, respectively. Small circles indicate Cu atoms on the level $z = -1/52$ or $1/52$ (corresponding to the level $z = \pm 1/4a'$). Cu atoms within the regions of Bi clusters are not drawn.

occupancies are 70.0%, and they are shifted from the ideal centers of the sulfur tetrahedra toward the centers of these equipoints along lines connecting the atoms and cluster centers. The displacement distances equal the distances between each center of the Cu complexes and the centers of the ideal Cu tetrahedral sites, multiplied by 0.028. Those Cu atoms occupying the triangular sites are given occupancies of 5.9% and are distributed randomly in the structure. Isotropic temperature factors of Cu atoms in the tetrahedral and triangular sites are 1.2 and 2.5 respectively.

S atoms. The S atoms form a cubic close packed framework. Those belonging to the regions of the Bi complexes, namely those which are within 9.8Å from the equipoints 4a, 4b and 24d are shifted in the same directions as the Bi atoms. On the other hand, the remaining sulfur atoms are regarded as belonging to the regions of the Cu complexes and are displaced in the same directions as the tetrahedrally-coordinated Cu atoms. The displacement distances are given by the values of the distances between the center of each complex and the centers of their ideal sites, multiplied by 0.02. Isotropic temperature factors are 0.8. Sulfur atoms are assumed to fully occupy their sites.

Discussion

Through our synthesis work, it has been found that one of the materials quenched from about 550°C in the compositional region of Cu_9BiS_6 reveals a non-integral type higher order structure that is based on the substructure corresponding to the cubic α-chalcocite. The superstructure determination has shown that the structure consists of periodically spaced clusters of Bi and of Cu; in a cubic close packed sulfur framework, one has a rocksalt-like structure of Bi and S, and the other has a α-chalcocite-like structure of Cu and S. These spherical clusters, each about 18Å in diameter, are alternately distributed according to a face-centered cubic arrangement. The metal clustering arrangement is schematically drawn in Figure 7.

The phenomenon of replacement between Bi and Cu atoms is of special importance, since it is a characteristic commonly observed in other materials in the Cu_2S–Bi_2S_3 system and is closely related to this modulated structure. In the refined substructure of the cubic phase (Fig. 3), Bi atoms occupy the centers of octahedral holes in the sulfur packing, and are partly replaced by Cu atoms. Cu atoms do not occupy the centers of the octahedra but are statistically distributed among four equivalent positions around centers of the tetrahedra and near the centers of the trigonal faces of the octahedra. Crystal-chemical characteristics of such an unusual replacement in the materials of this system are discussed in Tomeoka *et al.* (1980). According to Sugaki and Shima (1972), most compounds that reveal this replacement are stable only at high temperature and metastable at room temperature. The extra peaks observed in our study are not found in powder patterns above 400°C, where the crystals were synthesized, but they appear only when the material is quenched. $Cu_3Bi_5S_9$ is another of these materials, and when quenched from the stable high temperature phase, it also reveals non-integral type satellite reflections. These facts suggest that the quenched materials do not retain the structure of the high temperature stable phase. At high temperature, the crystal may exist with a disordered metal atom distribution that can be approximated by the substructure defined in this study, and may not reveal such higher order structure as observed in the quenched specimen.

Finally, the periodically spaced metal clusters that define this higher order structure can be considered to be produced in the process of quenching. In other words, when the crystal is quenched to room temperature, Bi and Cu atoms, which were mixed with each other in disorder, segregate into the two kinds of metal clusters, which occur alternately and periodically, and which produce this modulated structure. The phenomena seem to be very similar to those of "G–P zones" found in metal alloys. In the case of $Cu_3Bi_5S_9$, the atoms segregate as two-dimensional sheets parallel to (010), and the satellite reflections appear one-dimensionally in the direction of b*. The long-range repeat distances of both materials would be directly influenced by the size of these metal clusters and seem to change according to a change of composition.

Variation of the period and the periodicity of long-range ordering

The effect of shift modulation is remarkable in our material and can be understood as a result of static interaction between the metal atoms, which is caused by local clustering of Cu and Bi. On the one hand, Bi atoms are displaced from the ideal centers of the sulfur octahedra in the direction outward from the central positions of the Bi complexes, and on the other hand Cu atoms conversely move from the centers of the tetrahedral sites in the directions inward to the central positions of the Cu complexes. Thus, the shift modulation occurs in accordance with the substitutional modulation so that the local expansion and shrinkage of the clusters alternate in the arrangement of face centered cubic lattice points. In this way, the crystal minimizes the mutual interactions of the atoms and keeps the whole structure in equilibrium.

As indicated in Table 1, the repeat distance of the long-range ordering has a tendency to become longer, from 6.0 through 6.75, as the cell edge length of the substructure becomes longer. The change of cell edge length without changing basic substructure would be related to the change of the ratio Bi:Cu and suggests that the cubic phase has a solid solution range of some extent in the high temperature stable phase. Because Bi is a much bigger atom than Cu, an increase in the cell edge length would be consistent with an increase in the Bi content and a decrease in the Cu content. Since Bi and Cu atoms exist in clusters, an increase in the content of Bi implies expansion of the Bi clusters, and conversely a decrease in the content of Cu implies shrinkage of the Cu clusters. Considering that the repeat distance of long range ordering should be directly

influenced by the size of these metal clusters, it is reasonable that an increase in Bi content brings about the extension of the repeat distance of the superstructure.

The satellite spots are usually broad, compared with the main spots, and there is a noticeable difference in the broadness of the satellite spots among the different crystals (Table 1). In the extreme case, the reflections are too broad to be called spots. The satellite peaks have a tendency to become broader as the length of the cell edge decreases. The broadening of the peaks may be attributed to decreasing the regularity of long range ordering, whereas sharp main peaks indicate a regular arrangement of the substructure. In the refinement, the introduction of statistical replacement between Bi and Cu into the superstructure model greatly improved the agreement between FO and FC. This fact may be related to the broadening of satellite peaks and indicates that disordering of the metal complexes still occurs even in the low temperature superstructure.

Acknowledgments

We express our sincere gratitude for the guidance and encouragement received from Dr. Ryoichi Sadanaga. We also thank Drs. Yoshio Takeuchi, Hiroshi Takeda, Kazumasa Ohsumi and Takamitsu Yamanaka for valuable discussions during the course of this investigation, and Dr. Hiromi Shima for a discussion concerning the phase relationship in the Cu_2S–Bi_2S_3 system. We received helpful comments on this study from Dr. Howard T. Evans. The final version of the paper was improved by thorough reviews from Drs. Peter R. Buseck, David R. Veblen and Piers P. K. Smith. Computations were performed HITAC 8700/8800 at the Computer Center of the University of Tokyo.

References

Buhlmann, E. (1971) Untersuchungen im System Bi_2S_3–Cu_2S und geologische Schlußfolgerungen. Neues Jahrbuch für Mineralogie, Monatshefte, 137–141.

Coppens, P. and Hamilton, W. C. (1970) Anisotropic extinction corrections in Zachariasen approximation. Acta Crystallographica, A26, 71–83.

Cromer, D. T. (1965) Anomalous dispersion corrections computed from self-consistent field relativistic Dirac-Slater wave functions. Acta Crystallographica, 18, 17–23.

Donnay, G., Donnay, J. and Kullerud, G. (1958) Crystal and twin structure of digenite, Cu_9S_5. American Mineralogist, 43, 228–242.

Evans, H. T., Jr. (1971) Crystal structure of low chalcocite. Nature Physical Science, 232, 69–70.

Evans, H. T., Jr. (1979) The crystal structures of low chalcocite and djurleite. Zeitschrift für Kristallographie, 150, 299–320.

Frueh, A. J. (1953) An extension of the 'Difference Patterson' to facilitate the solution of ordered-disordered problems. Acta Crystallographica, 6, 454–456.

Guinier, A. (1963) X-ray Diffraction in Crystals, Imperfect Crystals, and Amorphous Bodies, p. 279–282. San Francisco, Freeman.

International Tables for X-ray Crystallography, Vol. 4 (1968), The Kynoch Press, Birmingham, England.

Koch, F. and Cohen, J. B. (1969) The defect structure of $Fe_{1-x}O$. Acta Crystallographica, B25, 275–287.

Koto, K. and Morimoto, N. (1975) Superstructure investigation of bornite, Cu_5FeS_4, by the modified partial Patterson function. Acta Crystallographica, B31, 2263–2273.

Morimoto, N. and Kullerud, G. (1961) Polymorphism in bornite. American Mineralogist, 46, 1270–1282.

Morimoto, N. and Kullerud, G. (1963) Polymorphism in digenite. American Mineralogist, 48, 110–123.

Morimoto, N. and Kullerud, G. (1966) Polymorphism on the Cu_5FeS_4–Cu_9S_5 join. Zeitschrift für Kristallographie, 123, 235–254.

Ohmasa, M. (1973) The crystal structure of $Cu_{2+x}Bi_{6-x}S_9$(x = 1.21). Neues Jahrbuch für Mineralogie, Monatshefte, 227–233.

Ohmasa, M. and Nowacki, W. (1973) The crystal structure of synthetic $CuBi_5S_8$. Zeitschrift für Kristallographie, 137, 422–432.

Ohmasa, M., Tomeoka, K. and Sadanaga, R. (1979) The modulated structure of $Cu_3Bi_5S_9$. AIP Conference Proceedings No. 53, 355–357.

Ozawa, T. and Nowacki, W. (1975) The crystal structure of, and the bismuth-copper distribution in synthetic cuprobismuthite. Zeitschrift für Kristallographie, 142, 161–176.

Roseboom, E. H. (1966) An investigation of the system Cu-S and some natural copper sulfides between 25° and 700°C. Economic Geology, 61, 641–672.

Sadanaga, R., Ohmasa, M. and Morimoto, N. (1965) On the statistical distribution of copper ions in the structure of β-chalcocite. Mineralogical Journal, 4, 275–290.

Sugaki, A. and Shima, H. (1971) The phase equilibrium study of the CuBiS system. Proceedings of the IMA-IAGOD Meetings '70, IMA Volume, Special Paper No. 1, 270–271.

Sugaki, A. and Shima, H. (1972) Phase relations of the Cu_2S–Bi_2S_3 system. Technology Reports Yamaguchi University, 1, 45–70.

Takeuchi, Y. (1972) The investigation of superstructures by means of partial Patterson functions. Zeitschrift für Kristallographie, 135, 120–136.

Tomeoka, K., Ohmasa, M. and Sadanaga, R. (1980) Crystal chemical studies on some compounds in the Cu_2S–Bi_2S_3 system. Mineralogical Journal, 10, 57–70.

Tomeoka, K. (1980) The modulated structures in the system of Cu_2S–Bi_2S_3. Doctoral thesis, University of Tokyo, Tokyo.

Wuensch, B. and Buerger, M. J. (1963) The crystal structure of chalcocite, Cu_2S. Mineralogical Society of America, Special Paper, 1, 164–170.

Wuensch, B. and Prewitt, C. T. (1965) Corrections for X-ray absorption by a crystal of arbitrary shape. Zeitschrift für Kristallographie, 122, 24–59.

Manuscript received, July 20, 1981;
accepted for publication, November 30, 1981.